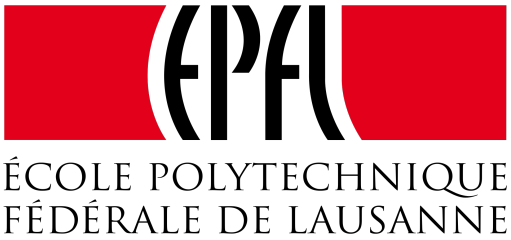

Advanced topics in first-principles electronic structure calculations

Lab 3

Atomistic and Quantum Simulations of Materials

Prof. Nicola Marzari

Laura Mismetti

Spring semester 2022

In this report several advanced aspects of DFT are studied, in particular the calculation of the electronic band structure of a solid (Calcium oxide in this case), density of states, projected density of states, augmentation of the standard DFT functionals to include van der Waals interactions, magnetic properties. The software Quantum Espresso (QE) has been used in all the calculations, together with ultrasoft pseudopotentials (USPP), in order to ease the computational cost with respect to the norm-conserving pseudopotentials.

1 Exercise 1: CaO band structure and DOS calculation

In this first exercise the goal is to compute the band structure and density of states of face-centered cubic (fcc) CaO. By band structure we mean the energy bands $E_n(\mathbf{k})$, eigenvalues of the energy that appear inside the Schrodinger equation, where $\mathbf{k}$ assumes the values that lie along a given path inside the first Brillouin Zone and n is the number of solutions of the Schrodinger equation at a given $\mathbf{k}$. In our case the chosen path is composed by the segments that connect the following high-symmetry points of the correspondent body-centred cubic (bcc) reciprocal lattice: W-L-Γ-X-W-K, with coordinates

$$\begin{aligned} &\Gamma = (0,0,0), \qquad X = \frac{2\pi}{a}(1,0,0), \qquad L = \frac{2\pi}{a}\left(\frac{1}{2},\frac{1}{2},\frac{1}{2}\right), \\ &W = \frac{2\pi}{a}\left(1,\frac{1}{2},0\right), \quad K = \frac{2\pi}{a}\left(\frac{3}{4},\frac{3}{4},0\right) \end{aligned} \tag{1}$$

The other quantity we are interrested in is the density of states (DOS), which is the number of states of the system in an infinitesimal interval of energy $[E, E+dE]$, it is then indicated as $D(E)$. Assuming that in our case there is spin degeneracy, the formula that leads to the DOS is:

$$D(E) = 2\frac{V}{(2\pi)^3}\sum_n \int_{\text{B.Z.}} \delta\left(E - E_n(\boldsymbol{k})\right) d\boldsymbol{k} \tag{2}$$

The calculation is then performed by using a numerical method to compute the integral of the delta functions inside the Brillouin zone, it is called the tetrahedra method.

In order to achieve the desired results a self-consistent field (SCF) calculation for the system is needed first, then starting from the equilibrated structure a non-self-consistent field (NSCF) calculation can be performed.

1.1 Task A

First of all we need to compute the ground state electronic density of the fcc CaO lattice. We use the primitive unit cell, composed by only two atoms, and with lattice parameters equal to

$$\boldsymbol{a}_1 = \frac{a}{2}(-1,0,1), \quad \boldsymbol{a}_2 = \frac{a}{2}(0,1,1), \quad \boldsymbol{a}_3 = \frac{a}{2}(-1,1,0) \tag{3}$$

where $a = 9.089\ a_0$ and $a_0 = 0.5291\mathring{A}$ the Bohr radius, also called atomic unit. The Calcium ion and the Oxygen one are then positioned at $(0,0,0)$ and $(a/2,0,0)$, respectively. A series of SCF calculations is required to test the convergence with respect to the kinetic energy cutoff. In addition, the use of ultrasoft pseudopotentials introduces the need to test the convergence also with respect to the charge density cutoff. However, the study of the convergence here is neglected and the values of the mentioned cutoffs are set to the ones found in the "Standard solid-state pseudopotentials library", which have been already tested.

$$\begin{aligned} E_{cut,Ca} &= 30\ Ry \\ E_{cut,O} &= 50\ Ry \\ \rho_{cut,Ca} &= 240\ Ry \\ \rho_{cut,O} &= 400\ Ry \end{aligned} \tag{4}$$

Then, in order to assure convergence, the highest values are chosen, so we set $E_{cut} = 50\ Ry$ and $\rho_{cut} = 400\ Ry$ for our calculations. The same has been done for the number of $\mathbf{k}$ sampling points in the Brillouin zone, and a value of 8 points in each direction has been used.

The SCF calculation gives a value of $-116.308\ Ry$ as ground state energy of the fcc CaO unit cell, while the highest occupied level by the electrons corresponds to $7.6144\ eV$. It also allows to store the ground-state density of the system and the self-consistent Kohn-Sham potential that we will need later.

1.2 Task B

Once the first SCF calculation has been performed, the band structure can be found by running the NSCF calculation, starting from the stored ground state. To do so, the command `'bands'` has been set in the input file to specify the NSCF type of the calculation, while the parameter `'nbnd'`, which represents the number of bands to compute, has a value of 28, as the number of electrons present in the unit cell (Ca has 20 electrons and O only 8). Indeed we are interested in both the conduction and valence bands.

The path W-L-Γ-X-W-K in the Brillouin zone is also specified in the input file, by choosing a finite number of sampling points for each segment. In particular, the chosen amount of **k**-points is proportional to the length of each segment:

$$\begin{aligned} W - L &= 40 \\ L - \Gamma &= 60 \\ \Gamma - X &= 80 \\ X - W &= 20 \\ W - K &= 20 \end{aligned} \tag{5}$$

The last step to obtain the plot of the energy bands as a function of the wave-vector, is to run the QE executable **bands.x**. Figure 1 shows the calculated band structure of CaO through the procedure described above, where the reference for the energies has been set to the highest occupied level of the valence band found before. As it is possible to see, we have calculated enough bands to be able to see both the valence band, that will be completely full, and the conduction band, which will be empty if the material is in its ground state. The two bands are also well separated, indeed there is an energy gap between them, which means that the material is an insulator.

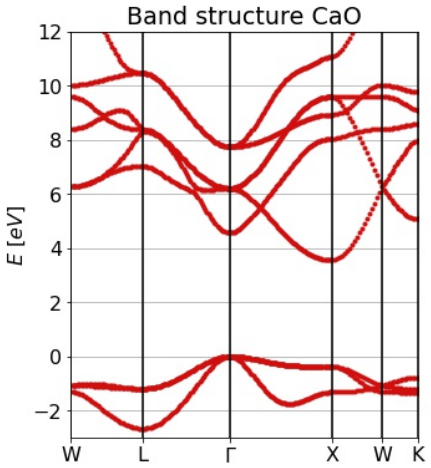

Figure 1: Energy bands of the fcc CaO lattice.

The analysis of the band structure reveals that the indirect energy gap of CaO is equal to 3.648 eV, which we remind is the energy difference between the maximum of the valence band and the minimum of the conduction band (also called HOMO-LUMO difference), it is called indirect because the two minima correspond to different wave-vectors **k**. It's possible to observe that this material has also a direct gap, indeed the conduction band has a local minimum in correspondence to

the maximum of the valence band. Its value is 4.826 eV. These values confirm what said before. Insulators with energy gaps around 1 $eV - 2$ eV are called semiconductors and have different properties than proper insulators. The material we are studying has larger energy gap than this, so it is an insulator.

At this point it's fundamental to compare the obtained results with what we find in the literature. Figure 1 in [1] and Figure 3a in [2] show a very similar pattern of the energy bands to the one we have found. The stationary points are in the same positions and each line seems to follow almost the same trend. In [1], by using GGA, the value of the indirect gap of CaO is found to be equal to 3.67 eV, while the indirect one is 4.79 eV. These values are both very close to ours, indeed both the relative errors are around 0.6%. Another comparison can be done also with the result found in [2], where the calculated indirect gap is 6.25 eV. This value is significantly larger than our, indeed they have used a different technique and it is more sophisticated: they employed the Tran-Blaha modified Becke-Johnson exchange potential (mBJ) to further improve the energy gap calculations and optical properties. At this point it's obvious that we get results closer to the values in [1], indeed we used the same technique as them. On the other hand, both our results and the ones in [1] are far from the values found in [2]. Indeed the addition of another term to the DFT functional makes the method more precise.

The last comparison needs to be done with the experimental value, which is equal to 7.1 eV for the indirect gap. This value is almost twice the one we have found, while it is close to the value reported in [2]. This shows that DFT is not very good at calculating excited states, indeed it's only a ground state theory. Only when some specific tools are added to DFT, like it has been done in [2], the prediction of the energy gap, which strongly depends on the excited states of the system, and other optical properties are satisfactory.

Finally, by computing the energy gap of the material, it's possible to understand if it has a specific colour or it is colourless. Once the material is excited, some electrons occupy the first excited state and they tend to decay to the ground state by emitting photons. If this photons have a wave-length in the range of the visible light, then the material appears to have a specific colour at our eyes. The allowed (more likely to happen) electronic transitions are the ones that involve the direct gap, indeed otherwise in the indirect gap the electron must exchange momentum with the lattice, which is far unlikely. Then, by considering the direct gap we have found, and the relation which describes the energy of a photon, we are able to predict the colour of CaO.

$$E_{photon} = h\nu \tag{6}$$

$$\lambda = \frac{hc}{\Delta E_{direct}} = \frac{4.13\ 10^{-15}\ eVs \cdot 3\ 10^{8}\ m/s}{4.826\ eV} = 256.7\ nm \tag{7}$$

We remember that the range of visible light is around $380\ nm - 700\ nm$. Then the decay of CaO electrons from the first excited state to the ground state emits photons with a wavelength that is close, but still smaller, than this range. CaO shouldn't have a specific colour and it appears white.

1.3 Task C

We want now to calculate the density of states of CaO. In order to do so, an additional NSCF calculation is required by setting a denser **k** points mesh than before, specifically we use 16 sampling points in each direction. From this calculation the Fermi energy of CaO results to be $9.431\ eV$.

Then the QE executable **dos.x** allows to easily calculate the DOS. Its input file contains the range of energies that we are interested in, which, by setting the reference value to the highest occupied level, is between $-3\ eV$ and $12\ eV$. The discretization bin is set to $0.1\ eV$.

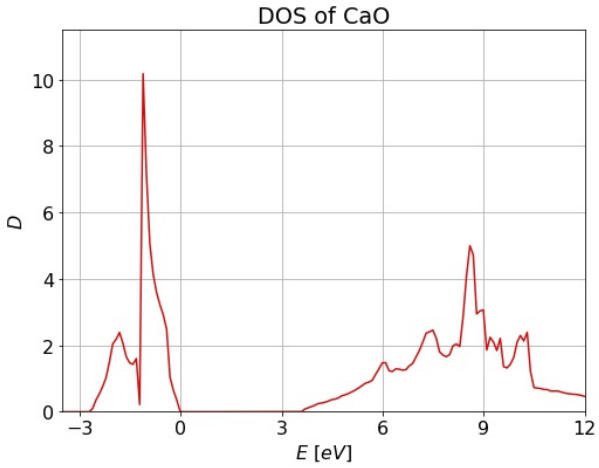

Figure 2: Density of states of the fcc CaO lattice, shifted by taking as reference the highest occupied level with energy $-7.6144\ eV$

Figure 2 shows the DOS of CaO and, as expected, it perfectly corresponds to the band structure found previously. Indeed, the DOS is different from zero only in energy regions where at least one energy band is present, while in correspondence of the energy gap (indirect in this case because it's the smallest) the DOS is zero. It's then possible to check the calculation of the energy gap by looking at the

density of states of the material. In this case the range of energies where the DOS is equal to zero is 3.64 eV, and it confirms our previous finding.

By using another QE executable, called **projwfc.x**, we easily obtain also the projected density of states (PDOS), which reveals the relative contribution of a particular atom or orbital to the total DOS.

As it is possible to see in Figure 3 the states close to the Fermi energy are mostly occupied by electrons of the Oxygen, while the conduction band is mainly composed by Calcium orbitals.

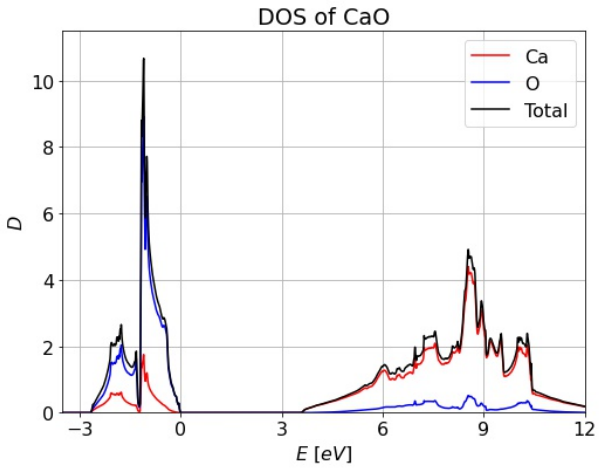

Figure 3: Projected density of states of the fcc CaO lattice for the two elements Ca and O.

It's also possible to separate all the single orbitals and study which ones contribute to the DOS for a certain energy. All the s-orbitals of Oxygen and s,p of Calcium give very small contribution to the valence band, indeed they are occupied by the core electrons and such bands are not shown here because we are not interested in them. More interesting are the p-orbital of O and d-orbital of Ca, indeed they give important contributions to valence and conduction bands (see Figure 4). The p-orbital of Oxygen is the one which contributes the most to the valence band close to the Fermi energy. It means that it is highly densely occupied. On the other hand, the conduction band is almost completely composed by the $3d$-orbital of Ca, that is empty (in the ground state). The electronic configuration of Oxygen and Calcium can be then deduced from here by considering the number of electrons that each element has. So for the Oxygen it is $[1s^2, 2s^2, 2p^4]$, while for Calcium it is $[1s^2, 2s^2, 2p^6, 3s^2, 3p^6, 4s^2]$. Consequently, we can understand that the 2 electrons of the Calcium in $4s$-orbital become of the Oxygen which is then able to complete the p-orbital. It's possible to recognize the ionic bond between Ca and O. In CaO the $2p$-orbital of the Oxygen is completely occupied and it compose

the valence band, while $4s$ and $3d$ of the Calcium are empty and constitute then the conduction band.

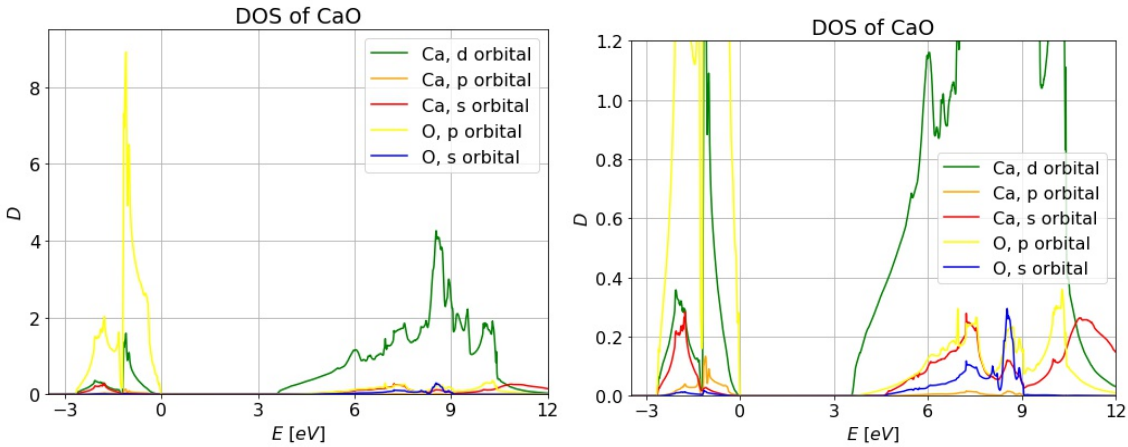

(a) PDOS of Ca and O orbitals

(b) Zoom of the range of D in $0 - 1.2$

Figure 4: Projected density of states of the fcc CaO lattice showing the contributions of different orbitals.

The magnetic order of the material depends on the number and disposition of the electrons in the orbitals. Each unit cell has an even number of electrons and all of them are paired, then they have antiparallel spins and by summing them the 'total spin' results to be zero. The system doesn't have magnetic properties.

2 Exercise 2: Structural optimization of h-BN

The goal of this second exercise is to find the optimal structure of Hexagonal Boron Nitride (h-BN), which means to determine its lattice constants. Then we also want to compute its band structure and density of states as in the previous exercise.

The structure of h-BN is made by layers of B and N atoms arranged in a honeycomb lattice. Two parameters are then necessary to describe such a structure: a, the in-plane lattice parameter, defines the atomic positions in every plane, and c governs the separation between the sheets. The Bravais lattice is clearly hexagonal with primitive lattice vectors equal to:

$$\boldsymbol{a}_1 = a(1,0,0), \quad \boldsymbol{a}_2 = a\left(-\frac{1}{2}, \frac{\sqrt{3}}{2}, 0\right), \quad \boldsymbol{a}_3 = a\left(0,0,\frac{c}{a}\right) \tag{8}$$

While the reciprocal lattice vectors, computed through the use of the relation $\boldsymbol{a}_i \cdot \boldsymbol{b}_j = 2\pi\delta_{ij}$, are:

$$\boldsymbol{b}_1 = \frac{2\pi}{\sqrt{3}}(\sqrt{3}, 1, 0), \quad \boldsymbol{b}_2 = \frac{4\pi}{\sqrt{3}}(0, 1, 0), \quad \boldsymbol{b}_3 = \frac{2\pi a}{c}(0, 0, 1) \tag{9}$$

The layers are held together by weak forces called van der Waals interactions. These are caused by the interactions between instantaneous dipoles generated by charge fluctuations inside the material. These fluctuations are the consequence of the quantum zero-point energy. The treatment of this kind of non-local correlations is critical in DFT, but it's indispensable to be able to predict correctly all the properties of such materials. Nevertheless, last foundings revealed that it's possible to take them into account by adding an additional non-local correlation term in the exchange DFT functional.

Later in this exercise we will study also the single layer h-BN, which is, as it's easy to imagine, a single sheet of h-BN. It can be interpreted as a usual h-BN structure with sheets infinitely far away from each other, which means the structure has a large enough c. We want to calculate optimal structure, band structure and density of states also in this case.

2.1 Task A

First of all, we calculate the optimal lattice parameters of h-BN and we can study them separately because they are weakly coupled. Then, we start by fixing c to the experimental value of $c_{exp} = 6.653$ $\mathring{A}$, as found in [3], and we calculate the ground state energy of the system by varying a by 0.01 a_0 in the range $[2.424\ \mathring{A}; 2.583\ \mathring{A}]$.

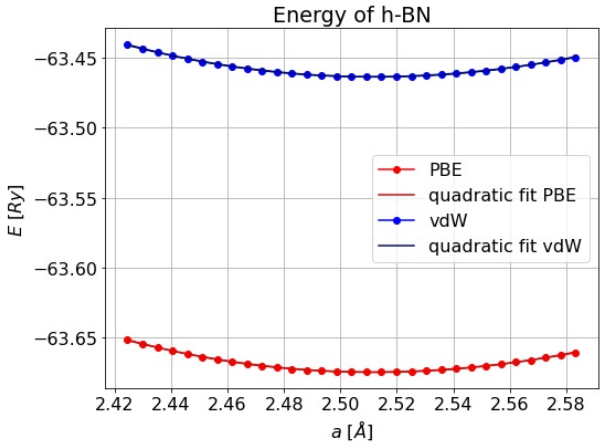

Figure 5: Ground state energy of h-BN while varying the in-plane lattice parameter a around the experimental value. It's calculated first through a PBE calculation and then by vdW-DFT. The relative fits are also shown.

In order to understand the effect of the van der Waals forces between the planes, the calculations are performed first without accounting for this kind of interactions, as it has been done until now, by performing pure PBE calculations. Then the van der Waals interactions are considered by inserting the command `input dft = 'VDW-DF'` in the input file. It allows to perform a PBE calculation with the vdW-DF correction: the extra non-correlation term is added to the exchange DFT functional.

When we are not taking into account the van der Waals interactions, so when we perform a normal PBE calculation, the minimum of the ground state energy corresponds to a value of the in-plane lattice parameter of $a = 2.5129$ $\mathring{A}$. While when the DFT functional takes into account this type of long-range interactions the minimum is reached at $a = 2.5113$ $\mathring{A}$.

To go on with our study we need to choose one of these two values. Then we take as reference the experimental value, $a_{exp} = 2.5047$ $\mathring{A}$ found in [3], and we choose the one which is closest to it. As it's easy to see, the value of a found by considering the vdW correction to tne DFT functional is closest to a_{exp} than the one obtained by performing PBE calculations. Then we set $a = 2.5113$ $\mathring{A}$ for the next calculations.

By looking at Figure 5, it's evident that the two curves are different from each other. The two have a very similar shape but the one which takes into account the van der Waals forces is slightly shifted upwards by approximatively 0.2 eV, which is quite small compared to the values of the energy (around -63.5 eV).

2.2 Task B

Now we can do the same study on c, which determines the separation between the layers. The range used for the parameter c is $[6.573\ \mathring{A}; 8.69\ \mathring{A}]$, while a is fixed as said before. The results found by performing PBE calculations are shown in Figure 6. It's possible to see that a minimum is present but it's not clearly defined. In addition, it is positioned around 7.5 $\mathring{A}$, which is far larger than the experimental value found in [3]: $c_{exp} = 6.653$ $\mathring{A}$. As expected from the theory, PBE calculations are not able to predict well the equilibrium structure of such materials.

On the other hand, if the van der Waals forces are taken into account, the situation changes dramatically, as shown in Figure 7. Here, the minimum of the curve is clearly visible, and a parabolic fit in that region allows to identify it precisely. It corresponds to $c = 6.485$ $\mathring{A}$, which is also closer to the experimental value.

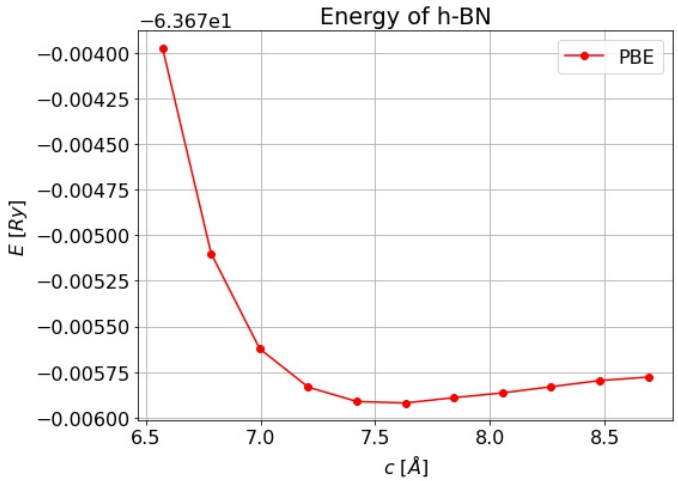

Figure 6: Ground state energy of h-BN, calculated through PBE calculations, while varying c.

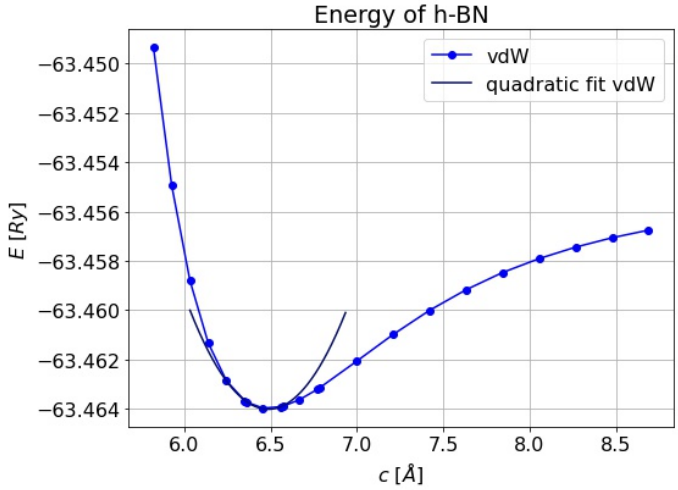

Figure 7: Ground state energy of h-BN calculated through vdW-DFT calculations, while varying c.

The van der Waals interactions then have effects on the ground state energy of h-BN as expected, in particular they are indispensable to calculate correctly the structure of systems composed by layers, like h-BN.

The equilibrium structure of h-BN has been calculated and it has $a = 2.5113$ $\mathring{A}$ and $c = 6.485$ $\mathring{A}$, and it is shown in Figure 8.

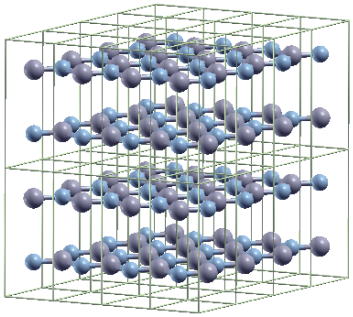

Figure 8: Repetitions of optimized hBN unit cell.

2.3 Task C

Starting from the optimized structure found before, we compute the band structure and the DOS of h-BN as it has been done in the first exercise. In this case the number of bands that we want to compute is set to 24, indeed the unit cell contains this amount of electrons, and it can be considered a good estimation to obtain both the conduction and the valence band.

The path in the Brillouin zone also needs to be set. As already described before, the reciprocal lattice of h-BN has a different shape from the one of CaO, indeed the high symmetry points are different. In this case we compute the integral along the path $K - \Gamma - M - K - H - A - L - H$, where the high symmetry points are defined as follows, in crystal coordinates.

$$\begin{aligned} &\Gamma = (0,0,0), \qquad K = \left(\frac{1}{3},\frac{1}{3},0\right), \quad M = \left(\frac{1}{2},0,0\right), \\ &A = \left(0,0,\frac{1}{2}\right), \quad H = \left(\frac{1}{3},\frac{1}{3},\frac{1}{2}\right), \quad L = \left(\frac{1}{2},0,\frac{1}{2}\right) \end{aligned} \tag{10}$$

The following band structure is obtained for h-BN, first by performing the usual PBE calculation and then adding the vdW term. The results are compared in Figure 9. It's possible to see that the two results are very similar to each other. This means that also PBE technique, if it starts from the equilibrium structure of the system, is able to predict well the energy bands.

By following the procedure illustrated in Exercise 1, we are able to reproduce also the density of states of h-BN in both cases.

Also in this case the two figures are very similar to each other. There is only a small difference in the conduction band of the DOS. Indeed the vdW case shows

a slightly higher number of states than the PBE one. So, also in this case we can conclude that the PBE calculation, starting from the equilibrated strucure, is able to predict correctly this property of the system, even if it's not taking into account the long-range interactions.

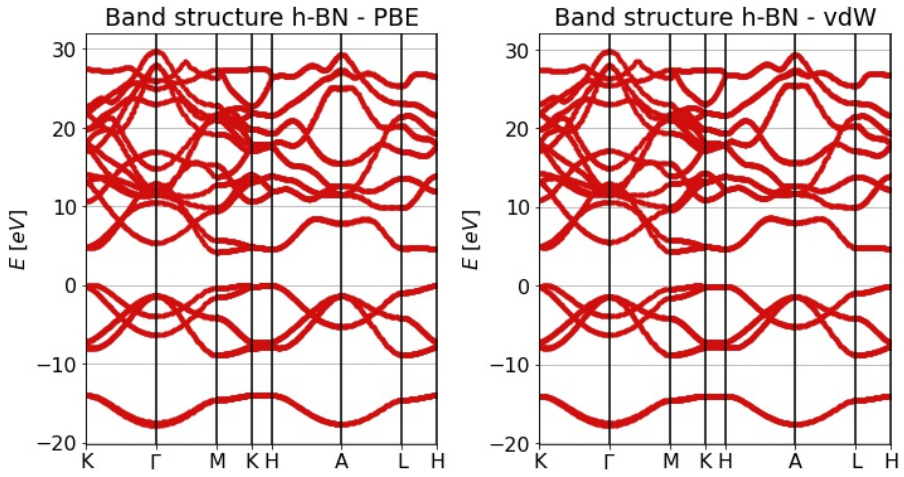

(a) Usual PBE calculation (b) vdW-DFT calculation

Figure 9: Energy bands of h-BN computed through different types of DFT calculations.

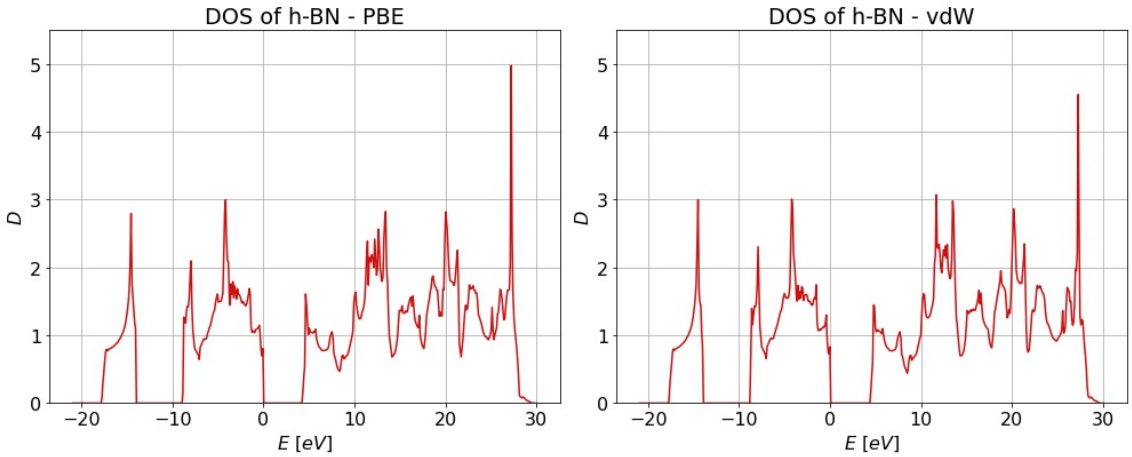

(a) Usual PBE calculation (b) vdW-DFT calculation

Figure 10: Density of states of h-BN computed through different types of DFT calculations.

2.4 Task D

In order to study the single layer h-BN, we need to start from the same structure as before and change the value of the lattice parameters. We want every sheet of h-BN to be isolated, it means that each plane shouldn't feel the presence of the others. In order to do so it's enough to set the lattice parameter c, to a big enough value. It can be calculated by looking at the ground state energy of the system while c increases. When the energy stops increasing, with respect to a threshold, it means that there is no more interaction between the planes. Due to the fact that there are van der Waals forces between the planes, we choose a threshold lower than the typical smallest values of these interactions (around 0.04 kJ/mol). The threshold is then set to 3 $10^{-5} Ry$.

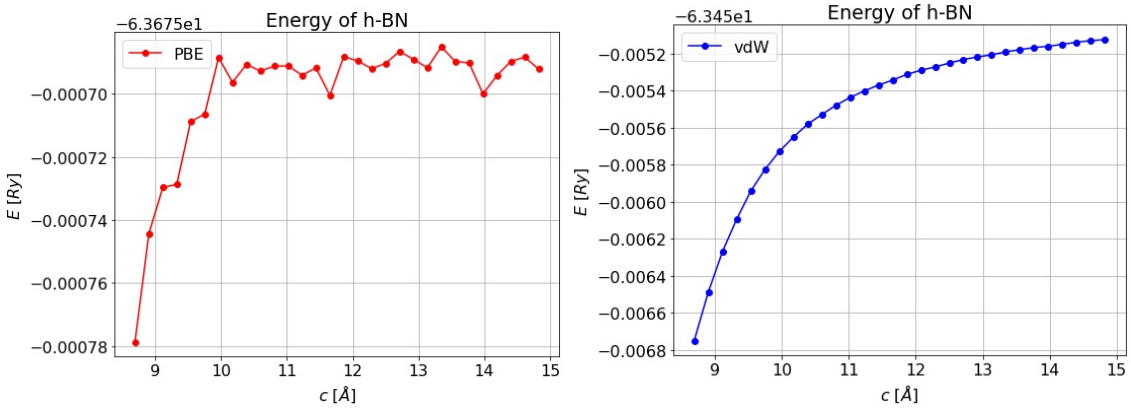

(a) Usual PBE calculation

(b) vdW-DFT calculation

Figure 11: Ground state energy of single layer h-BN computed through different types of DFT calculations, varying c.

By referring to Figure 11, a value of $c = 14$ $\mathring{A}$ is adopted, and it should be large enough in order to consider layers of h-BN that, even if there are the periodic boundary conditions, are not interacting with each other.

Then, due to the fact that we are considering a different structure from before, a new optimal value of a needs to be found. It's done by following the same procedure as for the total structure of h-BN.

As it's possible to see in the image the value of a at which there is the minimum of the energy is 2.511 $\mathring{A}$ in the case of PBE calculations, and 2.508 $\mathring{A}$ for vdW-DFT. The two values are very similar to each other and also very close to the value of a found for the entire h-BN structure. Indeed, we remember that the two parameters were weakly coupled, which means that one is not affecting the other. This calculation could have been easily avoided, by assuming that a is the same also in the case of single layer h-BN.

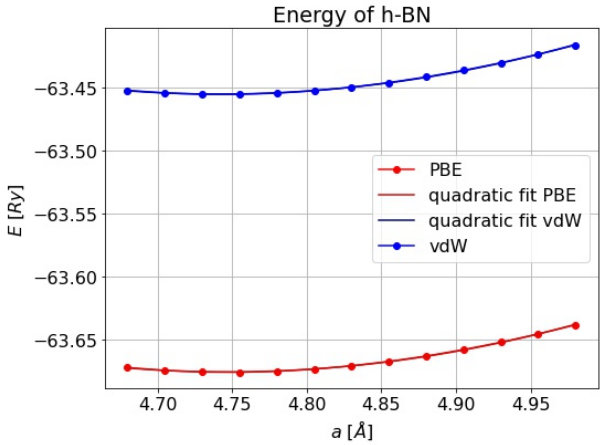

Figure 12: Ground state energy of single layer h-BN calculated through PBE and vdW-DFT calculations, while varying a. The relative fits are also shown.

The single layer hBN then appears as in Figure 13.

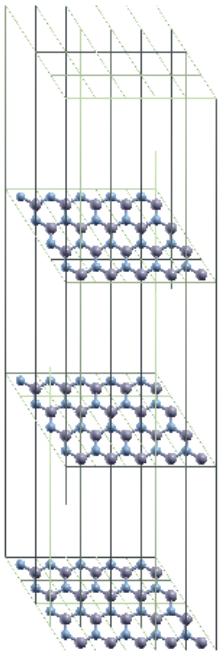

Figure 13: Repetitions of optimized single layer hBN unit cell.

2.5 Task E

Once we have found the optimal lattice parameters of the system, it's possible to proceed with the calculation of other properties, as we have already done in the case of bulk h-BN.

The band structure is computed along the path $K-\Gamma-M-K$, where the high symmetry points are defined as in Equation (10), indeed the shape of the unit cell of the lattice is always the same. What changes in this case is the number of atoms per unit cell, indeed they are only two, displaced in the same 'sheet'. We always assume that the number of electrons in the unit cell is a good estimation for the number of bands, in order to obtain half of them full and the other half empty. As a consequence, by calculating 12 bands of the single layer h-BN, both the valence and the conduction band are computed, as it is possible to see in Figure 14.

Also in this case the band structure is correctly predicted in both cases, with and without taking into account the van der Waals interactions. Indeed, the same explanation as before is valid: the usual PBE method is able to predict lattice properties correctly if the optimal structure is already known.

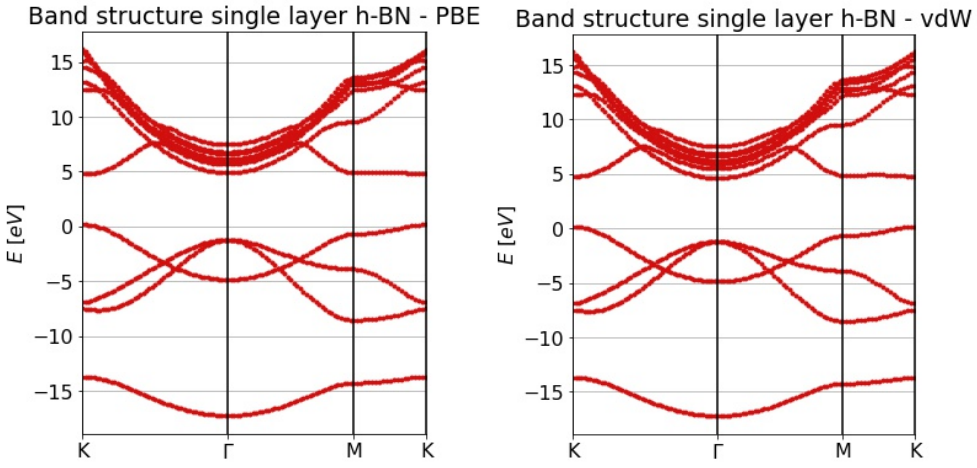

(a) Usual PBE calculation

(b) vdW-DFT calculation

Figure 14: Energy bands of single layer h-BN computed through different types of DFT calculations.

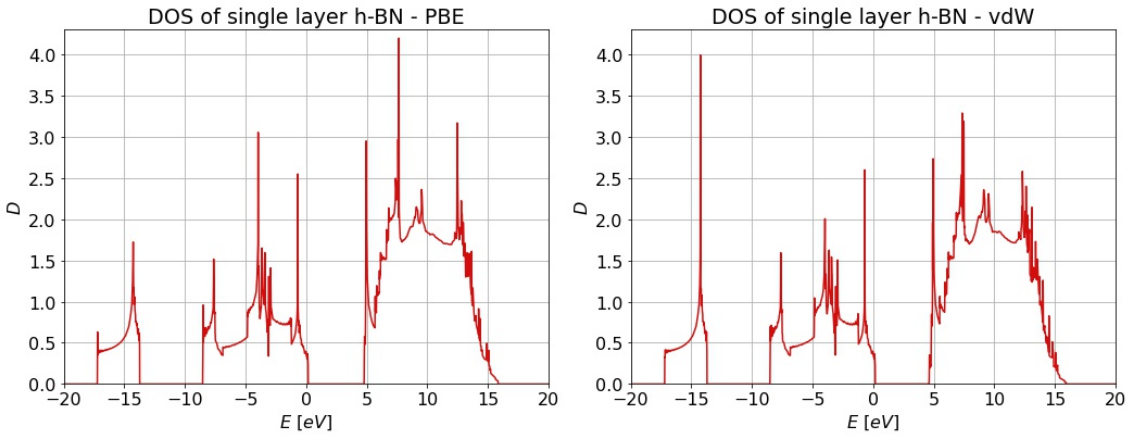

(a) Usual PBE calculation

(b) vdW-DFT calculation

Figure 15: Density of states of single layer h-BN computed through different types of DFT calculations.

On the other hand, the DOS in Figure 15 appear similar even if some relevant differences are present. The one calculated through vdW-DFT has a larger value for the states around $-15\ eV$, while both valence and conduction band have slightly smaller values. Although, also in this case both PBE and vdW-DFT are performing well, for the same reason as before.

At this point, we can compare the band structure of single layer h-BN with the first half of the band structure of bulk h-BN, indeed the first half of the path used for bulk h-BN corresponds to the entire path for single layer h-BN. The two valence bands look very similar, both for their shape and for the ranges of energies that they occupy. Quite different are instead the conduction bands.

By comparing Figure 10 and 15, it appears clear that both the DOS reflect what just observed for the band structure. The density of states in the valence band is quite similar in all the cases, while the conduction band of single layer h-BN has a larger amount of states close to the energy gap.

2.6 Task F

Now that both bulk h-BN and single layer h-BN have been studied, another quantity that relates them can be estimated. It's the energy per unit area necessary to break bulk h-BN into single sheets. To compute it we need to look at the energy to bring the different planes of bulk h-BN far away, until they don't feel each other anymore. This situation corresponds to have different sheets of isolated single layer h-BN, and it can be reached when the lattice parameter c of the structure is around 14 $\mathring{A}$. Then, the energy difference that there is between bulk h-BN with

the optimal c and with $c \sim 14$ $\mathring{A}$, is what we are looking for. Obviously then it needs to be normalized with the surface area of a unit cell.

So, referring to Figure 7 and 11, and knowing that the surface of a unit cell of our hexagonal lattice is $A_{unit\ cell} = 5.46\ \mathring{A}^2$, we have that the energy per unit area necessary to break bulk h-BN into sheets is around $0.00164\ Ry/\mathring{A}^2$.

$$A_{unit\ cell} = \frac{\sqrt{3}}{2}a^2 = \frac{\sqrt{3}}{2}(2.5113\ \mathring{A})^2 = 5.46\ \mathring{A}^2 \tag{11}$$

$$\begin{aligned}\Delta E = \frac{E_{sl\ hBN} - E_{bulk\ hBN}}{A_{unit\ cell}} = \frac{-63.455\ Ry - (-63.464\ Ry)}{5.46\ \mathring{A}^2} \\ = \frac{0.009\ Ry}{5.46\ \mathring{A}^2} = 0.00164\ \frac{Ry}{\mathring{A}^2} = 0.0224\ \frac{eV}{\mathring{A}^3}\end{aligned} \tag{12}$$

It's possible to compare this value with the surface energy of bulk Ag found in Lab 1. Its value was around $0.15\ eV/\mathring{A}^2$, which is at least one order of magnitude larger than the energy required to separate different planes of h-BN. We can interpret this result by remembering that the forces that keep different layers of h-BN together are van der Waals forces, and they are very weak, while Ag bulk is bonded through metallic bonds, which are, around one order of magnitude, stronger. So the fact that a higher energy is needed to create a surface in Ag bulk with respect to the energy required to separate a structure made by planes, kept together by van der Waals interactions, is perfectly reasonable.

3 Exercise 3: Iron stability under pressure and magnetism

In this last exercise we study another material, iron, which has interesting properties due to the fact that it's a metal. We are interested in computing its energy at different pressures when its atoms are arranged in two types of structure: BCC, body centered cubic, and HCP, hexagonal closed packed structure. In particular, first we focus on the geometry optimization of these structures and then we will study the transition pressure between these two phases. At the end the effects of magnetism on the ground state energy of BCC Fe will be studied.

All the calculations of this exercise are preformed by using the PBE exchange correlation functional already used in the previous exercises, so this information will be omitted later on. The wavefunction cutoff is always set to 55 Ry, while due to the fact that ultrasoft pseudo-potentials are used also a charge density cutoff is required and it's set to 240 Ry.

It's important to say that due to the fact that the material studied is a metal, it has magnetic properties. As a consequence, we need to take this feature into account when we perform our calculations. Even if we are not directly interested in studying them, they will affect the structure in a significant way. Then new parameters need to be defined to compute correctly the properties of iron. In the input file are added the following parameters:

- `nspin`: it defines the spin-polarization of the system. If a structure is non-magnetic it needs to be set to 1, while if we want to describe a ferromagnetic or antiferromagnetic state it should be equal to 2.
- `starting magnetization(1)=0.7`: it initializes the structure in a magnetic state (by referring to atomic type 1). In this way a magnetic ground state can be found through the procedure of optimization of the structure.
- `occupations='smearing'`: it introduces a fictitious temperature that allows the partial occupation of some states above the Fermi energy. In this way the integral over the Brillouin zone has a smoother integrand and it leads to smaller numerical errors.
- `smearing='m-v'`: it defines the type of function that we want to use for the smearing procedure. In this case it's the 'Marzari-Vanderbilt' function.
- `degauss=0.03`: it defines the spread of the smearing function. It's expressed in Rydbergs.

3.1 Task A

First of all, we study the geometry optimization of the two structures. As already said, the system of interest is a metal, and the parameters to define it appropriately are added into the input file as described in the previous paragraph. We also assume to already know the ground state magnetic order of the two structures. We start by considering the BCC structure, that has, as we already know, only one lattice parameter a.

In order to find the minimum of the ground state energy, the lattice parameter a has been varied in a range of $[2.11\ \mathring{A}; 3.57\ \mathring{A}]$ around the experimental value found in [4], $a_{exp} = 2.86\ \mathring{A}$.

The minimum is at $a = 2.836\ \mathring{A}$, which is very close to the experimental value found in the literature ([4]).

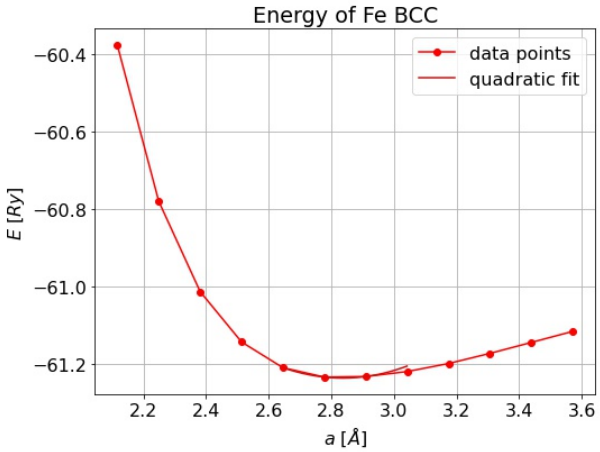

Figure 16: Ground state energy of Fe BCC varying a and relative parabolic fit.

The optimization of Fe HPC structure involves two parameters a and c, indeed the unit cell is hexagonal. Differently from what we have done for h-BN in the previous exercise, here we cannot optimize the two parameters separately because they are strongly coupled. We need then to perform more calculations by varying both of them at the same time. In order to do it easily it's possible to refer to the volume of the unit cell of the structure, that is showed in Figure 17 can be calculated through the following formulas.

$$V = c(2A_{triangle}) = c\left(2\frac{\sqrt{3}}{2}a^2\right) = \sqrt{3}a^2c = \sqrt{3}a^3\,(c/a) \tag{13}$$

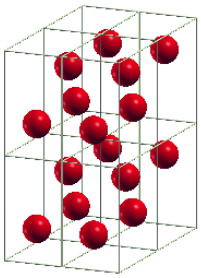

Figure 17: Some repetitions of Fe HPC unit cell.

The unit cell of an Hexagonal close packed structure indeed is not one of the fundamental Bravais lattice, it has 3 more atoms in the middle. Nevertheless, it can be obtained from the hexagonal Bravais lattice unit cell.

In order to find the minimum of the ground state energy we choose a range of volumes equal to $[18\ \mathring{A}^3; 22\ \mathring{A}^3]$. Then for each value we calculate the energy of the structure for different values of the ratio c/a in range $[1.4; 1.8]$. Indeed, once the volume V and c/a are fixed, also the parameter a, which is needed to define the structure in the input file, is fixed by the relation below, which comes from Equation (13).

A plot of the results obtained is shown in Figure 18.

$$a = \left(\frac{2}{\sqrt{3}}\frac{V}{c/a}\right)^{\frac{1}{3}} \tag{14}$$

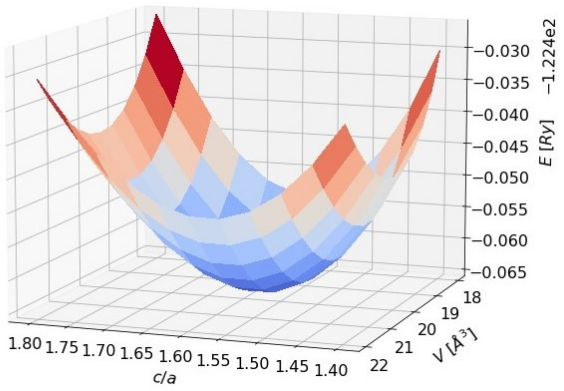

Figure 18: Ground state energy of Fe HPC varying the volume and the ratio c/a.

To find the optimal values for the parameters a, c a 3-dimensional fit is required. In particular, we use the data points around the minimum and we fit them with a paraboloid. It can be expressed as in Equation (15), but it also can be rewritten in the form of (16).

$$z = \left(\frac{x-c}{a}\right)^2 + \left(\frac{y-d}{b}\right)^2 \tag{15}$$

$$z = p_{00} + p_{10}x + p_{01}y + p_{20}x^2 + p_{11}xy + p_{02}y^2 \tag{16}$$

where x is the ratio c/a and y is the volume of the unit cell.

The least square method gives as best fit the curve shown in Figure 19 which has coefficients with values as in (17).

$$\begin{aligned} p_{00} &= -119.8\ Ry \\ p_{10} &= -1.664\ Ry \\ p_{01} &= -0.1342\ Ry/\mathring{A}^3 \\ p_{20} &= 0.5225\ Ry \\ p_{11} &= 0.0002237\ Ry/\mathring{A}^3 \\ p_{02} &= 0.003367\ \mathring{A}^6 \end{aligned} \tag{17}$$

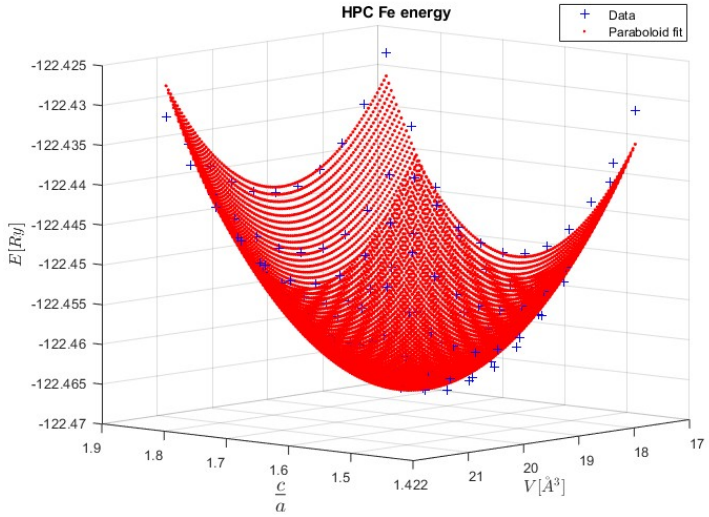

Figure 19: Fit of the data of Fe HPC ground state energy through a paraboloid.

The minimum is at $c/a = 1.58$ and $V = 19.87\ \mathring{A}^3$, so that $a = 2.44\ \mathring{A}$, and it has an energy equal to $E = -122.465\ Ry$. The experimental values reported in [5] are $a_{exp} = 2.45\ \mathring{A}$ and $c/a_{exp} = 1.60$. Then there is a very good accordance between our results and the experimental data.

3.2 Task B

Now that we have found the optimal parameters of both iron structures, we investigate the phase transition between BCC and HPC structure by looking at how their energies change with respect to the unit cell volume. We want to estimate the pressure at which this phenomenon happens when the temperature is 0 K.

It's important to remember that at the transition point the Gibbs free energy of the two structures is the same, so that it's possible to obtain the relation below.

$$\begin{aligned} G_{BCC} &= G_{HPC} \\ E_{BCC}(V_{BCC}) + V_{BCC}P &= E_{HPC}(V_{HPC}) + V_{HPC}P \end{aligned} \tag{18}$$

So, in order to do this the plots of the energies of BCC and HCP structures are needed as a function of volume. In the first case, for the BCC structure, we can simply find the volume as the cube of the lattice parameter a, so that the curve found in the previous task can be re-used. As we have already seen, the HCP structure instead has a more complicated geometry and in order to find a simple curve for the energy as a function of the volume the ratio c/a needs to be fixed. We choose then the value found previously, $c/a = 1.58$. By plotting both the curves on the same graph it's possible to see that there is an overlap at a certain point, which means that one structure becomes more favourable than the other. But it happens only at high pressures. Indeed, the BCC structure is the most favourable in normal conditions, indeed its minimum has a lower energy than the other one. But by changing the volume, and so the pressure, at a constant temperature, we allow the HCP to become the one with the lowest energy.

The pressure can be expressed as (19), so it's possible to obtain the value of the pressure at the transition point by applying the Maxwell construction of the common tangent. The equations of the tangent lines of both the curves have been found, and the angular coefficient of the one which is common to them (and with negative value, so that we obtain a meaningful value for the pressure) reveals the pressure.

$$P = -\frac{dE}{dV} \tag{19}$$

As it is possible to see in Figure 20, there is effectively a tangent which is in common between the two curves, and it has a slope that corresponds to $P = 20.68\ GPa$. The experimental value is around 13 GPa, according to [6]. So our result is similar, even if we are overestimating this quantity.

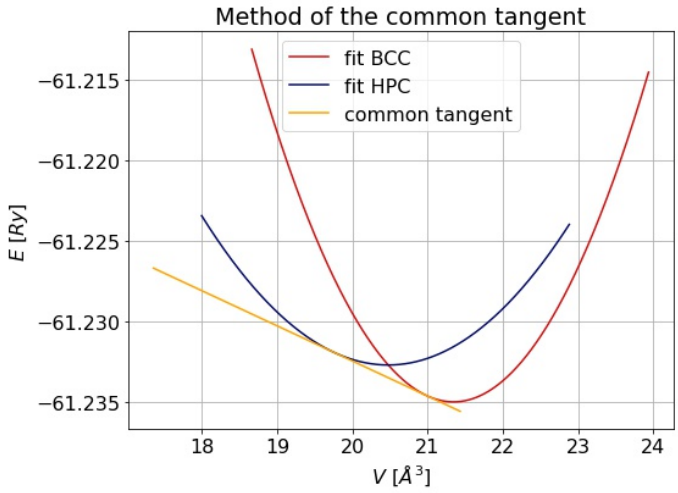

Figure 20: Method of the common tangent applied to BCC and HCP Fe structures.

3.3 Task C

Our last aim is to study the different magnetic states of BCC iron: ferromagnetic, anti-ferromagnetic and non-magnetic state. In particular we are interested in their ground state energy, density of states and projected density of states. As already said at the beginning of the exercise, we are treating a material with magnetic properties, and as a consequence special parameters have been defined inside the input file in order to capture its behaviour in a good manner.

We start from the ferromagnetic state of BCC iron. It requires the parmeter `nspin` to be set equal to 2, to be able to describe the two possible spin-polarizations of the system. It's easy to notice that this structure has already been studied, indeed in Task A we assumed to know the ground state of BCC Fe to be ferromagnetic. However, here we have calculated the energy in a smaller range of values of a, $[2.6\ \mathring{A}; 3.0\ \mathring{A}]$. The results are shown in Figure 21.

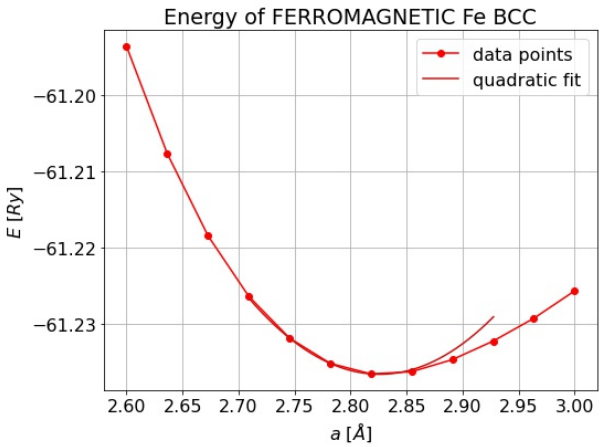

Figure 21: Ground state energy of BCC ferromagnetic iron as a function of the lattice parameter a.

In order to define the non-magnetic structure, we only have to change `nspin=1` and `starting magnetization(1)=0`. Indeed in this way the spin-up and spin-down of the system are not distinguished and the material is not spin polarized. The same range of parameters of the ferromagnetic BCC structure has been studied and the results are reported below.

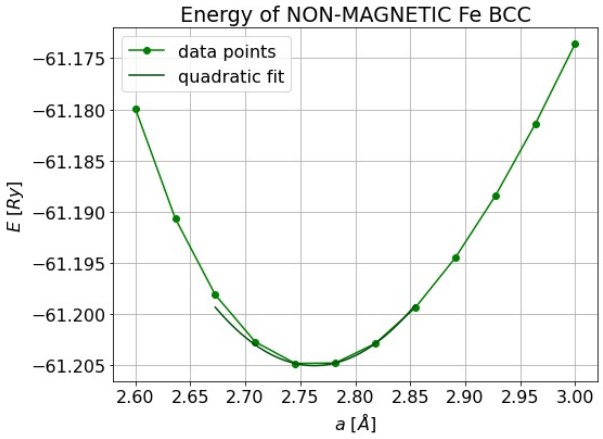

Figure 22: Ground state energy of BCC non-magnetic iron as a function of the lattice parameter a.

The last type of magnetic configuration we want to study is the anti-ferromagnetic one. In order to define it we need to specify two different types of Fe atoms, and assign to them opposite starting magnetization. Indeed in the input file of these calculations we have the atomic species `FeU`, Fe atoms with spin up, and `FeD`,

Fe atoms with spin down. And respectively `starting magnetization(1)=0.7`, `starting magnetization(2)=-0.7`. As in the previous cases we compute the energy for values of a in $[2.6\ \mathring{A}; 3.0\ \mathring{A}]$, as it is possible to see in Figure 23.

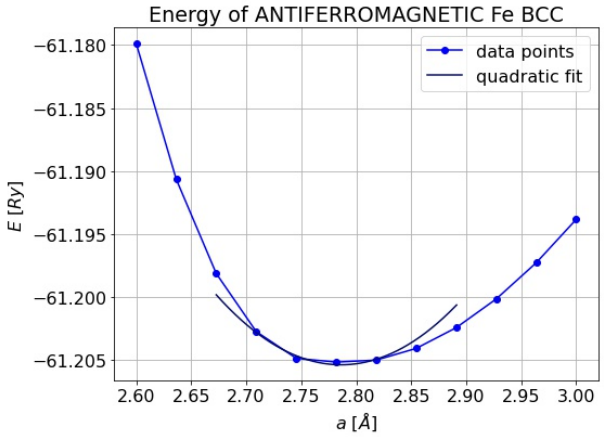

Figure 23: Ground state energy of BCC antiferromagnetic iron as a function of the lattice parameter a.

Now that all the structures has been optimized we can compare their ground state energy. In Figure 24 it's possible to see that the three curves have their minima in different positions and the correspondent energies are also different. In particular the ferromagnetic structure is the one with lowest energy, as reported in (20). Antiferromagnetic and non-magnetic BCC iron have more similar values of energy, but the antiferromagnetic structure has a slightly lower energy than the non-magnetic one. Also the positions of their minima are quite close to each other. Consequently, we can confirm that the most favourable magnetic structure of Fe BCC is the ferromagnetic one, with a lattice parameter of $a_{FER} = 2.826\ \mathring{A}$.

$$\begin{aligned} E_{FER} &= -61.2366\ Ry,\ a_{FER} = 2.826\ \mathring{A} \\ E_{NON-MAG} &= -61.2050\ Ry,\ a_{NON-MAG} = 2.762\ \mathring{A} \\ E_{AFM} &= -61.2053\ Ry,\ a_{AFM} = 2.786\ \mathring{A} \end{aligned} \tag{20}$$

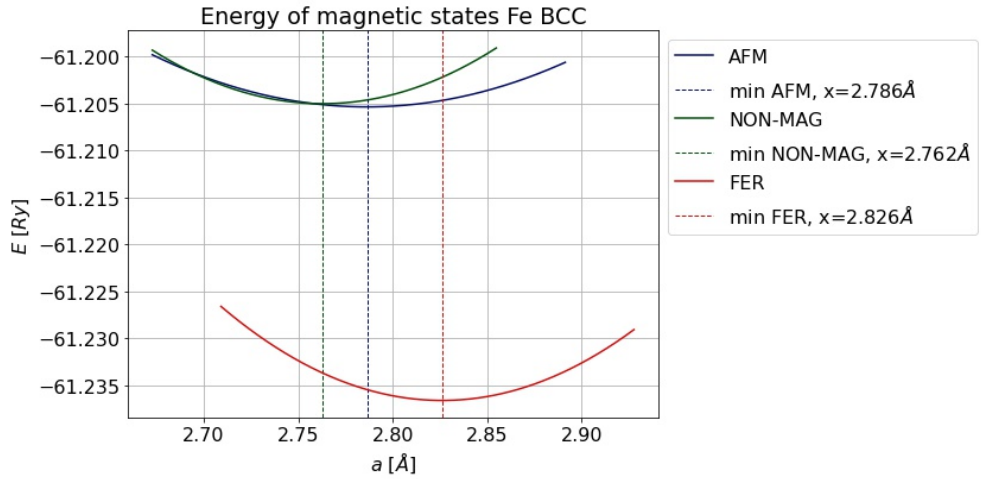

Figure 24: Ground state energy of different magnetic states of BCC iron as a function of the lattice parameter a.

The last thing we want to investigate is the density of states (DOS), and the projected one (PDOS), of these magnetic structures. After setting the lattice parameter to the optimal one found before, for each structure a NSCF calculation with a finer grid of **k**-points has been performed, and the DOS and PDOS calculated through the executables **dos.x** and **projwfc.x**.

First of all, it's important to notice that all the magnetic states of Fe have no energy gap between the valence and the conduction band. This is obviously a consequence of the fact that iron is a metal, so the electrons can move inside the material and they can easily go into the conduction band. There isn't a specific amount of energy that is required to excite the material.

As it is possible to see in Figure 25, in the ferromagnetic case, the two systems with spin-up and spin-down don't give the same contribution to the total DOS. Electrons with spin-up contribute more significantly at energies around 10 eV, while the ones with spin-down have an important contribution for slightly higher energies, around 15 eV. The total DOS then is concentrated in that range of energies, 10 $eV - 15$ eV.

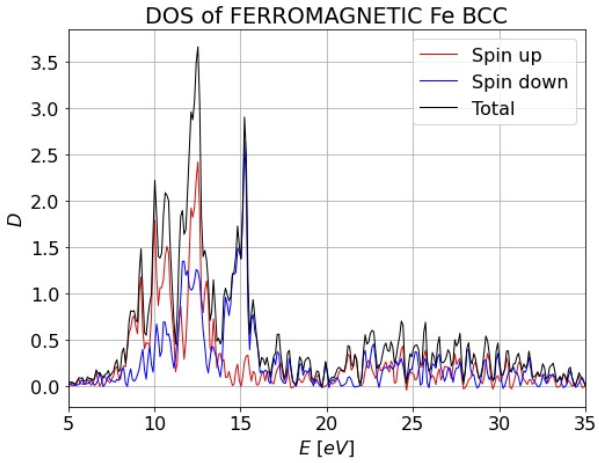

Figure 25: Density of states of ferromagnetic Fe BCC.

The non-magnetic case is instead quite different. Indeed, there isn't a distinction between spin-up and spin-down, the system is considered with paired spin. Then it's possible to look only at the total DOS of the system, where we know that the respective spin-up and spin-down electrons are giving the same contribution to it.

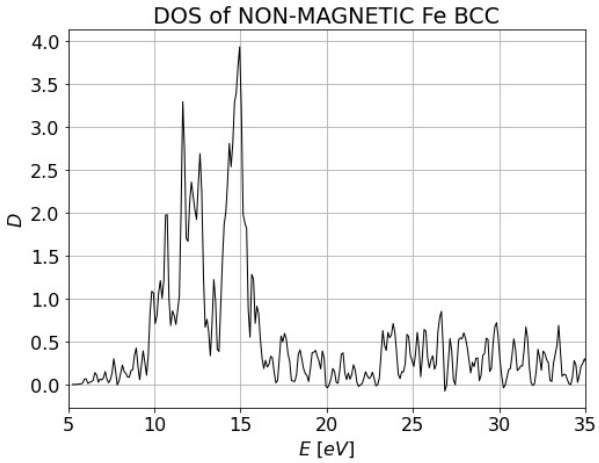

Figure 26: Density of states of non-magnetic Fe BCC.

Antiferromagnetic Fe BCC shows a very similar structure of DOS, which is concentrated between 10 eV and 15 eV. Although, the contributions of spin-up and spin-down systems are exactly the same in this case, and it can be explained by their antiparallel alignment inside the material.

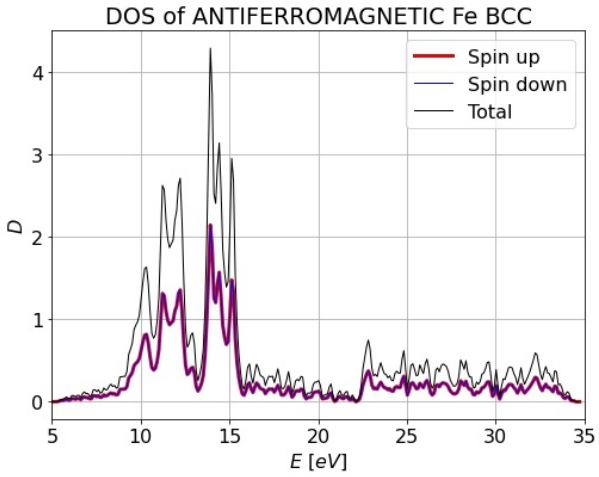

Figure 27: Density of states of antiferromagnetic Fe BCC.

By looking at the projected density of states it's also possible to understand which orbitals are contributing more to the DOS. In the case of iron, due to its electronic configuration, we are interested in the valence orbitals $4s$, $4p$, $3d$. As it is possible to see in Figures 28-29-30, the main contribution to the DOS is given by the $3d$-orbital in all cases, while $4s$ and $4p$ have contributions always lower than 0.5. Also in the PDOS it's possible to recognize the different contributions of electrons with spin-up and spin-down for ferromagnetic and antiferromagnetic Fe BCC, and the total DOS is then obtained by summing them. While, as already said before, we can't distinguish these two systems for the non-magnetic case.

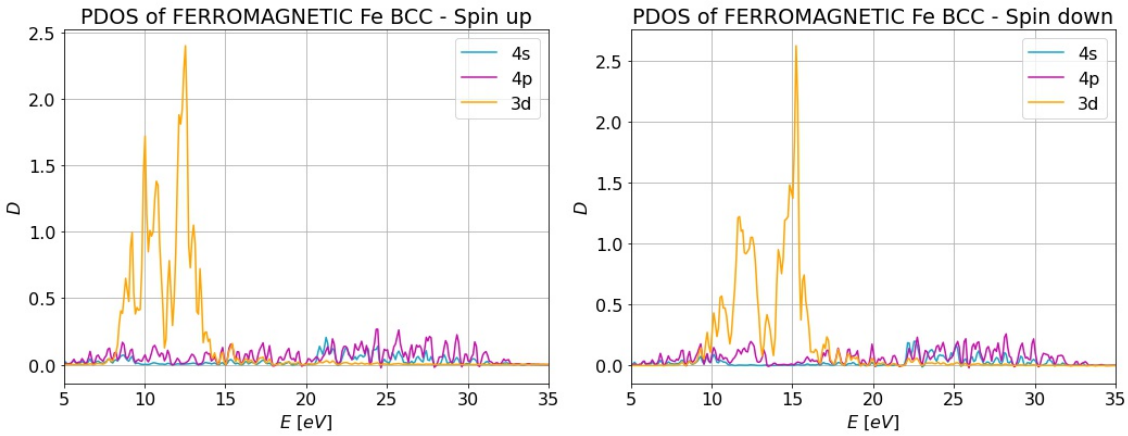

(a) Spin-up (b) Spin-down

Figure 28: Projected density of states of ferromagnetic Fe BCC.

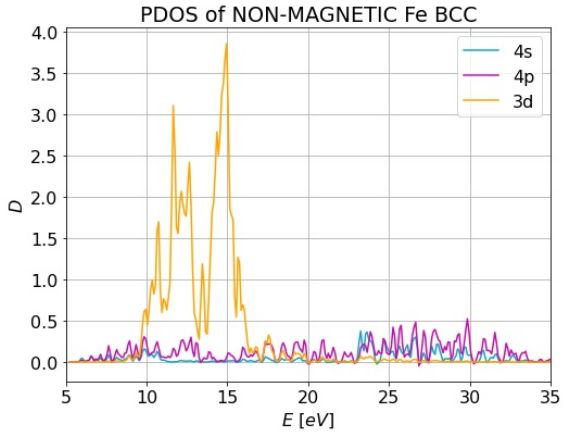

Figure 29: Projected density of states of non-magnetic Fe BCC.

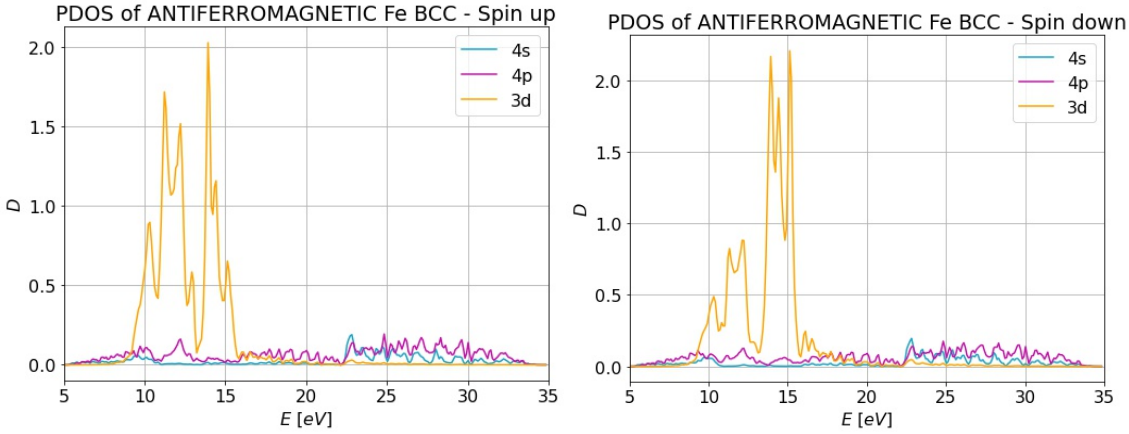

(a) Spin-up (b) Spin-down

Figure 30: Projected density of states of antiferromagnetic Fe BCC.

References

[1] E.L. Albuquerque and M.S. Vasconcelos, *Structural, Electronics and Optical Properties of CaO*, Journal of Physics: Conference Series 100 (2008) 042006

[2] Duy Khanh Nguyen, Vo Van On, D.M. Hoat, J.F. Rivas-Silva, Gregorio H. Cocoletzi *Structural, electronic, magnetic and optical properties of CaO induced by oxygen incorporation effects: A first-principles study*, Physics Letters A 397 (2021) 127241

[3] W. Paszkowicz, J.B. Pelka, M. Knapp, T. Szyszko, S. Podsiadlo *Lattice parameters and anisotropic thermal expansion of hexagonal boron nitride in the 10–297.5 K temperature range*, Appl. Phys. A 75, 431–435 (2002)

[4] Z.S. Basinski, W.H. Rothery and A.L. Sutton *The lattice expansion of iron*, Proc. R. Soc. Lond. A 229, 459 (1955)

[5] F. M. Wang and R. Ingalls *Iron bcc-hcp transition: Local structure from x-ray-absorption fine structure*, Phys. Rev. B 57, 10 (1998)

[6] M. Friák and M. Šob *Ab initio study of the bcc-hcp transformation in iron*, Phys. Rev. B 77, 174117 (2008)